JOURNAL OF GEOPHYSICAL RESEARCH, VOL. 102, NO. B8, PAGES 17,857–17,873, AUGUST 10, 1997

Crustal structure along the west flank of the Cascades, western Washington

Kate C. Miller, G. Randy Keller, and James M. Gridley

Department of Geological Sciences, University of Texas at El Paso

James H. Luetgert and Walter D. Mooney

U. S. Geological Survey, Menlo Park, California

Hans Thybo

Geological Institute, University of Copenhagen

Abstract. Knowledge of the crustal structure of the Washington Cascades and adjacent Puget Lowland is important to both earthquake hazards studies and geologic studies of the evolution of this tectonically active region. We present a model for crustal velocity structure derived from analysis of seismic refraction/wide-angle reflection data collected in 1991 in western Washington. The 280-km-long north-south transect skirts the west flank of the Cascades as it crosses three tectonic provinces including the Northwest Cascades Thrust System (NWCS), the Puget Lowland, and the volcanic arc of the southern Cascades. Within the NWCS, upper crustal velocities range from 4.2 to 5.7 km s^{-1} and are consistent with the presence of a diverse suite of Mesozoic and Paleozoic metasediments and metavolcanics. In the upper 2–3 km of the Puget Lowland velocities drop to 1.7–3.5 km s^{-1} and reflect the occurrence of Oligocene to recent sediments within the basin. In the southern Washington Cascades, upper crustal velocities range from 4.0 to 5.5 km s^{-1} and are consistent with a large volume of Tertiary sediments and volcanics. A sharp change in velocity gradient at 5–10 km marks the division between the upper and middle crust. From approximately 10 to 35 km depth the velocity field is characterized by a velocity increase from ~6.0 to 7.2 km s^{-1}. These high velocities do not support the presence of marine sedimentary rocks at depths of 10–20 km beneath the Cascades as previously proposed on the basis of magnetotelluric data. Crustal thickness ranges from 42 to 47 km along the profile. The lowermost crust consists of a 2 to 8-km-thick transitional layer with velocities of 7.3–7.4 km s^{-1}. The upper mantle velocity appears to be an unusually low 7.6–7.8 km s^{-1}. When compared to velocity models from other regions, this model most closely resembles those found in active continental arcs. Distinct seismicity patterns can be associated with individual tectonic provinces along the seismic transect. In the NWCS and Puget Lowland, most of the seismicity occurs below the base of the upper crust as defined by a seismic boundary at 5–10 km depth and continues to 20–30 km depth. The region of transition between the NWCS and the Puget Lowland appears as a gap in seismicity with notably less seismic activity north of the boundary between the two. Earthquakes within the Cascades are generally shallower (0–20 km) and are dominated by events associated with the Rainier Seismic Zone.

Introduction

Cascadia, located in the Pacific Northwest of the United States, is renowned for the snow-capped Cascade volcanoes that give the region its name. These volcanoes, while picturesque, pose great geological hazards from eruptions and cataclysmic avalanches. Their existence also serves as a reminder of the active subduction of the Juan de Fuca plate beneath the continental margin. This subduction has produced catastrophic earthquakes, not only along the plate boundary between the oceanic and continental plates but within the deforming overriding North American plate [*Atwater,* 1987; *Ludwin et al.,* 1991].

Presently, 10 million people live in the greater Cascadia region in cities and towns concentrated in the lowlands of the Puget Sound of Washington State and the Willamette Valley of Oregon (Figure 1). This growing urban corridor, which includes Portland, Seattle, and Vancouver, British Columbia, is sandwiched between the Cascades volcanoes to the east and the subduction zone to the west. Given the evident geological hazards in this region, the U.S. Geological Survey has placed increasing emphasis on scientific investigations that provide the structural framework in the Pacific Northwest. The present study uses seismic refraction and earthquake

Paper number 97JB00882.
0148-0227/97/97JB-00882$09.00

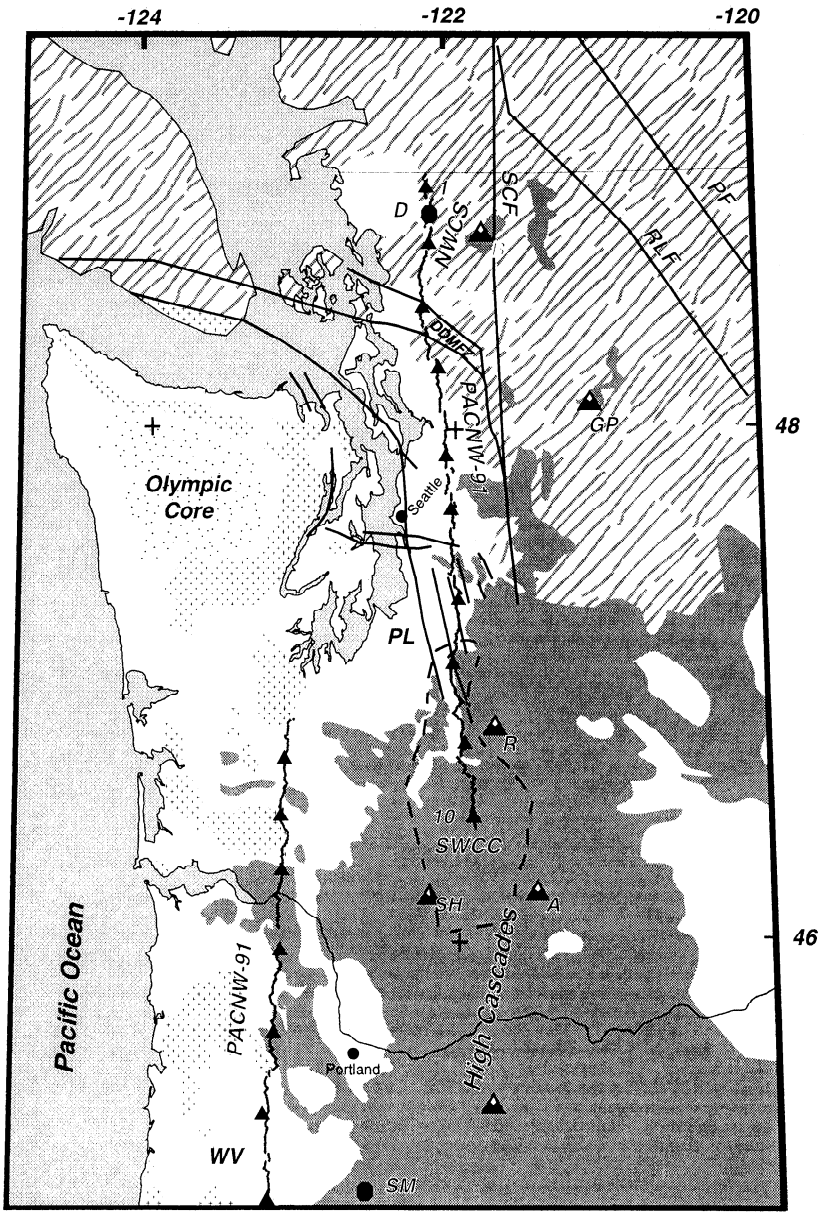

Figure 1. Index map to study area. Seismic surveys conducted in 1991 are annotated with solid triangles for shot points and tiny crosses for station locations. Shot points 1 and 10 are labeled for the northern deployment discussed here. Southern deployment is discussed by *Tréhu et al.* [1994]. Simplified geology after is keyed as follows: gray lines, pre-Tertiary rocks, including Northwest Cascades System (NWCS) rocks; dark gray, Tertiary volcanic rocks of the Cascades arc; small crosses, Eocene Crescent/Siletz rocks; stipples, Cretaccous–Paleocene accretionary prism sediments; white, Pliocene–Holocene sediments. Other symbols: white–topped triangles, arc volcanoes; solid lines, faults; dashed line, outline of Southwest Cascades Conductor (SWCC); solid octagons, earthquake epicenters for Deming (D) and Scotts Mills (SM) events. Other abbreviations: A, Mount Adams; B, Mount Baker; GP, Glacier Peak; R, Mount Rainier; SH, Mount St. Helens; DDMFZ, Darrington Devils Mountain Fault zone; PACNW–91, lines from experiment discussed in paper; PF, Pasayten Fault; PL, Puget Lowland; RLF, Ross Lake Fault; SCF, Straight Creek Fault; SCoRe, Southern Cordillera Refraction Experiment; SF, Seattle Fault, WV, Willamette Valley.

travel times to define the crustal structure at the boundary between the Cascades and Puget Lowland of Washington State as a contribution to establishing the deep geological framework of this region.

Geological Setting

The geologic evolution of western Washington is largely the product of oblique convergence between North America and the Juan de Fuca plates. This convergence has resulted in a complex forearc/volcanic arc terrane made up of many accreted blocks. Sediments, oceanic ridges, seamounts, and island arcs transported by the subducting plate have collided with, and been subducted or accreted to, the North American plate.

The oldest rocks in the study area are found in the Northern Cascades, which are composed of high-grade metamorphic rocks that

were amalgamated through accretionary processes in the late Mesozoic through mid-Tertiary times [*Misch,* 1988].

The modern Cascade Range is the product of the most recent episode of volcanism that has occurred along the margin of North America since the late Paleozoic [*McBirney,* 1978]. Much of the early geologic history is unknown due to the extensive late Cenozoic volcanic cover. Late Cenozoic volcanism in the Northern Cascades is largely limited to stratovolcanoes at Mount Baker and Glacier Peak.

From Mount Rainer south, the Cascade Range has typically been considered to consist of two subprovinces. The Western Cascades are predominantly mid-Miocene in age, with a pulse of activity in late Miocene time [*McBirney,* 1978]. Block faulting separated the Western Cascades from the High Cascades, the subprovince that includes all the major Quaternary stratovolcanoes.

Lying to the west of the Cascade Range, the Puget–Willamette Lowland is a discontinuous set of basins extending from Puget Sound to southern Oregon. In Washington, the basin is filled with sedimentary sequences eroded from the Olympic Mountains during Miocene uplift and during Pleistocene glaciation [*Tabor,* 1972; *Cady,* 1975]. The north-south trending Puget Sound portion of the lowland is cut by east-west striking folds and faults estimated to be of mid-Cenozoic age, which in most cases are buried by the sedimentary sequences [*Johnson,* 1984; *Johnson et al.,* 1994].

The Olympic Mountains and Coast Ranges of Washington and Oregon consist mainly of Eocene oceanic sediments and basalt [*Cady,* 1975]. The sediments in the Olympic Mountains are Eocene and younger subduction deposits that have been uplifted since late Miocene time and were accreted to the continent during subduction [*Tabor,* 1972; *Brandon and Calderwood,* 1990]. The Coast Ranges consists primarily of basalts [e.g., *Snavely et al.,* 1968] which may constitute a crustal block as thick as 30 km [*Tréhu et al.,* 1994], commonly termed the Siletz terrane. Paleomagnetic data from 62–12 m.y. old rocks of the forearc, arc and back arc indicate that large clockwise rotations of crustal blocks (15°–80°) have occurred in Washington and Oregon [*Wells,* 1990]. These rotations were likely driven by the oblique subduction, which was accommodated in the upper crust by strike-slip faulting.

Previous Seismic Studies

Prior to this study, no crustal-scale seismic refraction data were available for the western Cascades margin and Puget Lowland. *Crosson* [1976] estimated the crustal velocity structure beneath the Puget Sound basin from the inversion of local earthquake travel time data and obtained a crustal thickness of 41 km with a *Pn* velocity of 7.7 km s^{-1}. In the central Cascades, *Schultz and Crosson* [1996] obtained a crustal thickness of 48 km beneath the mountain range. South of our study area, *Leaver et al.* [1984] obtained a crustal thickness of 44 km for the Oregon Cascades and also found low (7.6 km s^{-1}) *Pn* velocities. West of our study, *Taber and Lewis* [1986] presented a crustal cross section across the Washington Coast Ranges at 47°N that showed the crust thickening from about 25 km at the coast to about 40 km beneath the southern Puget Lowland. A feature that is common to all of these models is the existence of relatively high crustal velocities (6.6–7.1 km s^{-1}) below 10 km depth. *Mooney and Weaver* [1989] reviewed previous geophysical work in the Pacific Northwest and presented a contour map of crustal thickness that included a 40-km-thick crust beneath the Washington Cascades based on the results of *Crosson* [1976] and *Leaver et al.* [1984].

Data Acquisition

In September 1991, the U.S. Geological Survey collected refraction/wide-angle reflection data along three profiles in western Washington and Oregon, in conjunction with the University of Texas at El Paso, Oregon State University, the Geological Survey of Canada (GSC), the University of British Columbia, and the University of Wyoming [*Luetgert et al.,* 1993]. Along the north-south profile in western Washington, approximately 485 vertical component seismic recorders and 20, three-component instruments were deployed at approximately 600-m intervals from the U.S./Canadian border near Mount Baker south through the Puget Lowland to Mount. Rainier (Figure 1). In addition, two high-resolution spreads of instruments were deployed. West of Mount Rainier near shot point 8 (Figure 1), a 192-channel two-component reflection spread was laid out at 200–m receiver intervals. Between shot points 2 and 3, a three-component array of 60 receiver at 50-m spacing was deployed using Program for Array Seismic Studies of the Continental Lithosphere (PASSCAL) Reftek instruments. The receivers recorded 10 dynamite shots, ranging in size from 900 to 1800 kg that were located at approximately 30-km intervals along the transect. During the experiment, an additional north-south profile was shot in southwestern Washington and northwestern Oregon, and an east-west profile was obtained in Oregon at the latitude of the city of Corvallis. Velocity models for these profiles are given by *Tréhu et al.* [1994].

Data Analysis and Modeling

Records for shot points 1 and 10 (Figure 2) illustrate the primary seismic phases seen in the data. In order to enhance signal to noise ratio and phase continuity in the data, individual shot records were bandpass filtered from 1 to 20 Hz and plotted with different amplitude corrections. First arrivals were usually identifiable on trace-normalized records out to distances of 200–250 km. Near the source, the first arrivals result from waves traveling in shallow sediments and volcanics, but the first arrivals soon become a true *Pg* phase, that is a diving wave which travels in the crystalline upper crust. At offsets less than 20 to 30 km, the first arrivals have apparent velocities of 3 to 5 km s^{-1}. Beyond 30 km, apparent velocities rapidly approach values of 6 to 6.5 km s^{-1} that are normally associated with the *Pg* phase. On the northern third of the profile, at offsets of only 20 km, the first arrivals locally exhibit large travel time advances and apparent velocities of about 7 km s^{-1}, where the overall moveout is of the order of 5 km s^{-1}. These arrivals suggest localized pods of high-velocity material in the upper crust.

A striking feature of the data is that at offsets beyond ~150 km the first visible seismic energy has an apparent velocity of ~7 km s^{-1}. Because ray paths for wide-angle reflections from an interface and diving waves penetrating to the vicinity of the interface are so similar, two possible interpretations of this observation are (1) the energy represents the far-offset branches of wide-angle reflections from the lower crust and Moho or (2) it represents diving waves traveling in the lower crust. In either case, *Pn*, the refracted phase from the upper mantle, is either absent or of such low amplitude that it falls below the ambient noise level. We tested both possible interpretations of the ~7 km s^{-1} phases. In addition, we obtained constraints on Moho depth and *Pn* velocity from earthquake arrival times. In the end, the same geological conclusion is drawn regardless of the interpretation chosen for the ~7 km s^{-1} phases. That is, the crust–mantle boundary in this region is extremely transitional.

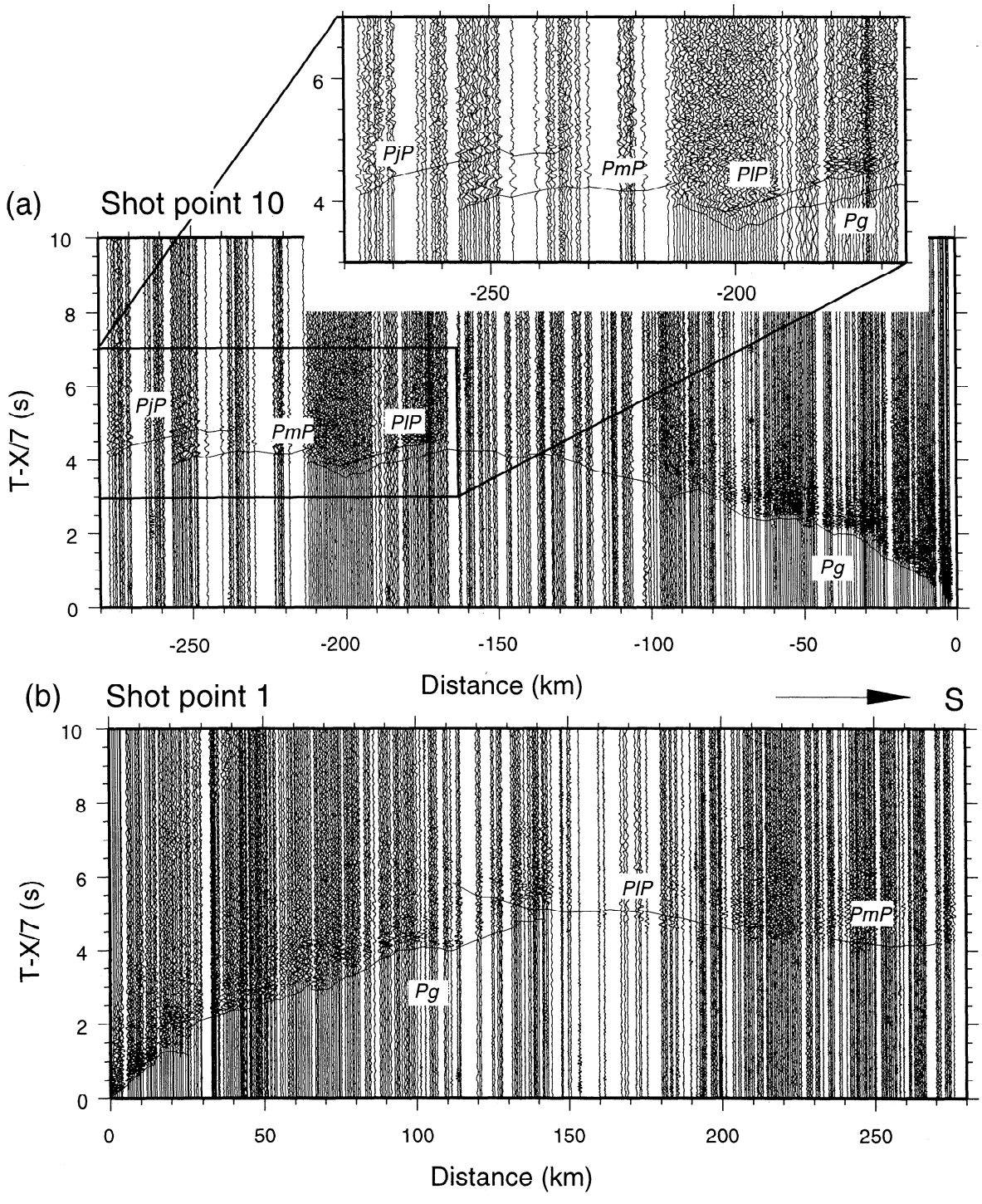

Figure 2. Trace normalized plots of shot record for (a) shot point (SP) 10 and (b) SP 1. Records have been filtered with a 1–20 Hz bandpass and are plotted with travel time reduced at 7 km s^{-1}. First arrivals were usually identifiable on trace–normalized records out to distances of 150–200km. In addition, there are secondary arrivals beyond 150 km offset which we interpret to represent wide–angle reflections from the lower crust and Moho.

Inversion of First Arrivals for Crustal Velocity Structure

To obtain a model for the crustal velocity structure along the profile (Plate 1), a tomographic inversion was performed with a least squares, nonlinear algorithm [*Hole*, 1992] that uses a finite difference solution to the eikonal equation [*Vidale*, 1990] to calculate travel times for first arrivals. The velocity model was calculated at a 1x1 km grid, except in the final iteration where a 0.5 x 0.5 km grid was calculated in order to improve accuracy. To diminish nonlinear effects of the inverse problem, the inversion was carried out as a "double-iterative" procedure. First, the maximum offset in the inversion was increased in successive steps starting at 40 km and increasing to 80, 120, 160, 200, and 285 km, the maximum offset in

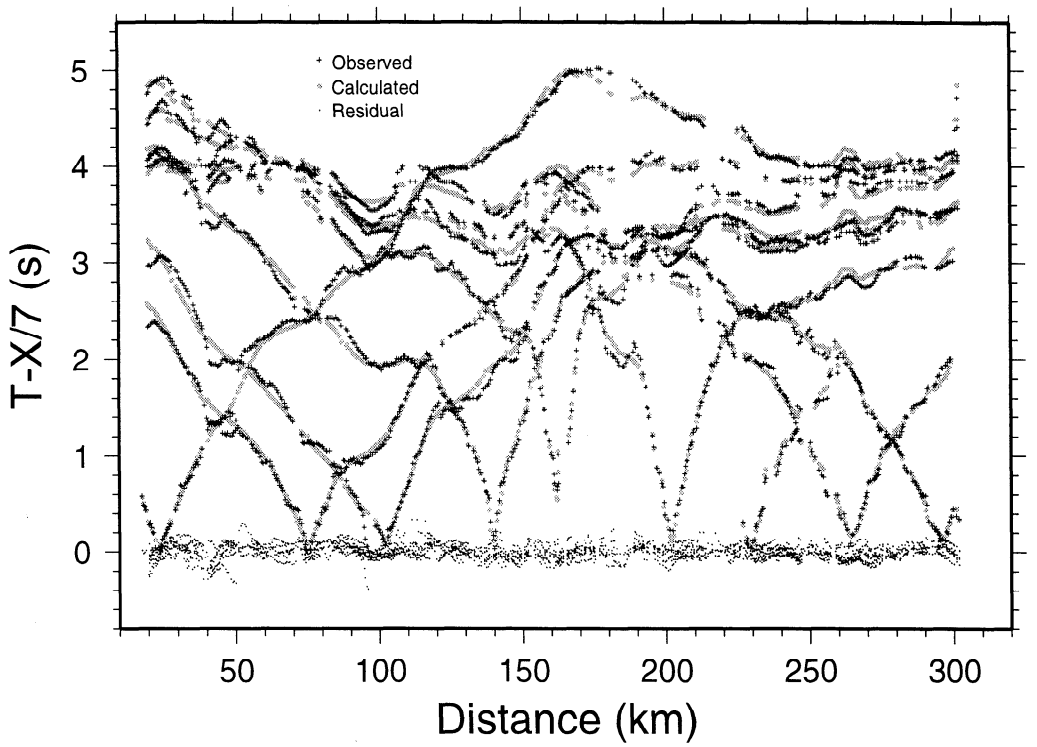

Figure 3. Observed travel times plotted against calculated and residual times from the tomography. Travel times are reduced by 7 km s^{-1}. Localized large travel time advances (e.g. at ~40 km on the plot) are poorly fit by the calculated travel times. As a result, velocities in this region are probably underestimated. Apparent velocities of ~7 km s^{-1} to offsets of 250 km require crustal thickness greater than 42–46 km.

the shot records. This corresponds to carrying out the interpretation "from top to bottom," thus further decreasing nonlinear effects in the algorithm. The second part of the double-iterative procedure consisted of reducing the size of the smoothing operator in five steps from 120 x 12 km to 8 x 2 km. This stabilized the inversion by distributing travel–time residuals over larger parts of the model for the longer smoothing operators and only allowing steep velocity gradients in later iterations with shorter smoothing operators for each offset interval [*Hole,* 1992]. Tests showed that the resulting model was independent of the initial model employed. The root-mean-square travel time residual for the final model is 75 ms (Figure 3), which represents a compromise between travel time fit, resolution, and nonlinearity.

In addition to the tomographic approach of *Hole* [1992] described above, an independent model for the upper 15 to 20 km of the crust was developed from first arrival times using the inversion algorithm of *Zelt and Smith* [1992] in combination with forward ray tracing [*Luetgert,* 1992], [*Gridley,* 1993]. The velocity models obtained from these different approaches produced similar results for the upper 15 to 20 km of the crust. However, we found that the methods of *Zelt and Smith* [1992], did not reproduce strong lateral heterogeneities in the velocity of the upper crust as well as the tomographic method of *Hole* [1992]. This was evident in the higher root-mean-square travel time residual obtained in the Zelt and Smith inversions (~150 ms) and the need to perform forward modeling to reduce these residuals. These differences are probably related to the way in which ray tracing is parameterized in the method of *Cerveny et al.* [1977] in the case of *Zelt and Smith* [1992] and [*Luetgert,* 1992], as compared to the finite difference solution to the eikonal equation [*Vidale,* 1990] in the case of *Hole* [1992]. In this paper, we have chosen to present the results from the tomographic inversion, as they elucidate details of the upper crustal velocity structure that are not as readily apparent in the other modeling effort. These details are evident in the 1-km grid used in the tomographic inversion, but not in the methods of *Zelt and Smith* [1992] which generally requires 10 to 20 km average node spacing required to maintain stability. Some details of geologic interest were also investigated further by forward ray tracing. Modeling of the middle to lower crust proceeded through inversion of reflected arrivals using the *Zelt and Smith* [1992] code and forward raytracing of *Pn* arrivals.

Modeling of Lower Crust and Upper Mantle Velocity Structure

Since the *Pn* phase was not clearly observed in the explosion data, the final model for the velocity structure of the lower crust and upper mantle is based on interpretation of wide-angle reflections in the explosion data, amplitude modeling employing the reflectivity method [*Fuchs and Müller,* 1971], and refracted phases from the upper mantle observed in earthquake arrival times at stations near the seismic profile. Our final model is consistent with the long-wavelength component of the gravity field and other seismic results in the area.

The final velocity model for the middle and lower crust (Plate 2) was obtained by fixing the velocities in the upper 10 km of the crust and inverting for the depth to reflecting horizons and the velocity above those horizons using the method of *Zelt and Smith* [1992]. The first step in this procedure was to convert the "pixel" style model parameterization of the upper crust from the tomography to the layer/velocity gradient parameterization required by *Zelt and Smith* [1992]. We did this by finding large velocity gradients in the tomographic model and using these as a guide to defining layers. These rapid changes in velocity were found by treating the model as an image and taking its Roberts gradient [e.g., *Gonzalez and Wintz,*

1987]. This operator is commonly used as an edge detector in image processing. In this case, rapid changes in velocity are pinpointed in the model. As might be expected, strong lateral velocity variations in the upper few kilometers of the model lead to the definition of at least two or three distinct layers. In addition, the procedure highlights another layer at 7 to 10 km depth. Velocities at the top and base of these layers were then defined at 10-km intervals based on the tomographic model.

At offsets beyond 150 km, secondary arrivals and a portion of the apparent first arrival energy are interpreted as reflected phases from either the lower crust or Moho. As a general statement, these phases are difficult to pick on any given record, but when all the records and the earthquake data are considered together, we found that three reflected phases, termed *PlP*, *PmP*, *PjP*, could be consistently identified. These phases are best seen on shots 1 and 10 (Figure 2) where energy from a lower crustal reflector (*PlP*) is seen from approximately 150 to 220 km, before it is overtaken by a second reflection between 220 and 300 km offset which we interpret to be *PmP*, the reflection from the crust mantle boundary. On the record for shot 10 (Figure 2, inset), between 240 and 280 km at 4.5–5.5 s, lies a third reflection which could correspond to a reflection from the top of the subducting Juan de Fuca plate *PjP*.

The first step in the inversion for lower crustal structure was to find a model to fit the *PlP* travel times. The starting model here consisted of three fixed layers that extended to depths of 7 to 10 km. The geometry and velocity structure of these layers were based on the tomographic results. In addition, velocities at the top of the fourth layer were held fixed based on the tomographic inversion. Velocities at the base of this layer and an interface initially placed at 35 km were allowed to vary. The initial depth of this interface and the velocity gradient in the layer were based on the tomographic inversion and some preliminary ray trace modeling. After obtaining an inverse solution which fits the travel times to an rms residual of 148 ms, a number of different starting models were tried to test the sensitivity of key aspects of the solution. A major feature of the final solution was that the interface at about 35 km domed up in the north central part of the model. Further inversion runs showed that if this interface was placed at shallower depths, the ends were depressed by the inversion: if it was placed deeper, the middle moved upward. Thus the general configuration shown in Plate 2 and Figure 4, in which the depth to this interface ranges from 32 to 38 km is robust, but the uncertainty in the depth at any point is estimated to be $\pm$ 2km. Also, the character of the reflected phases from this feature was complex and discontinuous suggesting that a single interface is a simplistic representation of the actual structure. The velocities in the layer are represented by a gradient from approximately 6.1 km s^{-1} (constrained by the tomography) to 7.2 km s^{-1} at the base of the layer (Plate 2 and Figure 4). These velocities are mostly constrained by the tomographic inversion (Plate 1). The inversion required that the velocity at the base of the layer be about 7.2 km s^{-1}, but considerable lateral variation could be tolerated. The velocity structure depicted in Plate 2 should be thought of as the simplest which fits the data.

With the upper four layers fixed, *PmP* travel times were modeled by allowing the velocities and the depth to the base of the crust to vary. This resulted in a fit with an rms residual of 150 ms. Moho depths range from 39 km on the north to 47 km to the south (Plate 2 and Figure 5). Velocities in the layer above the Moho range from 7.3 to 7.4 km s^{-1}. This velocity value was not very sensitive in the inversion, but the polarity and amplitude of the reflections from the top of this basal layer, *PlP*, indicate that a modest velocity increase was present. The values shown in Plate 2 are constrained so that such a velocity increase exists all along the top of the layer. The depth to the Moho was not highly sensitive to the velocity structure

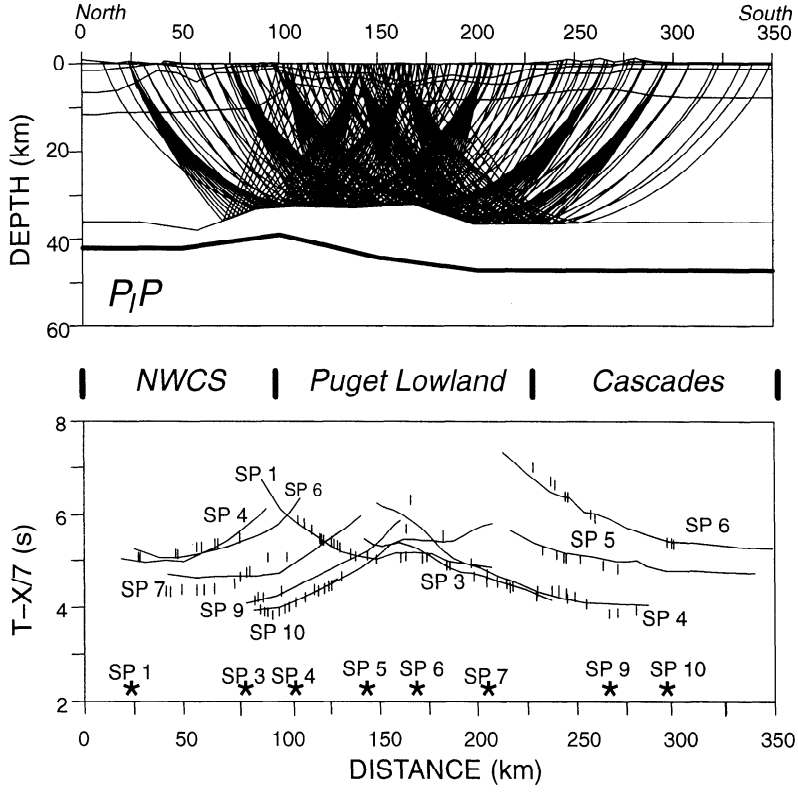

Figure 4. Ray trace diagram for the inversion of the *PlP* phase. Vertical bars are the observed travel times, and their height reflects the estimated uncertainty in the picks.

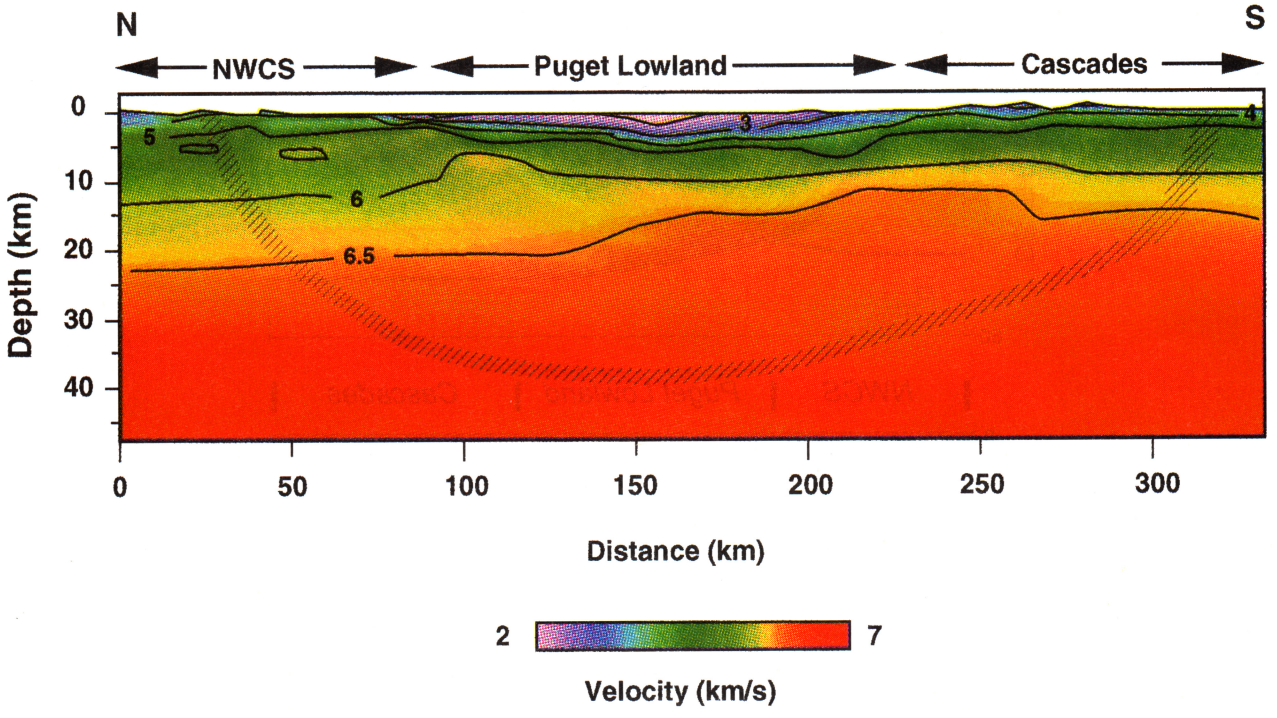

Plate 1. Tomographic velocity model. Velocities are contour 1 km s^{-1} intervals with the addition of a 6.5 km s^{-1} contour. Hachured region marks maximum depth of ray coverage for diving waves.

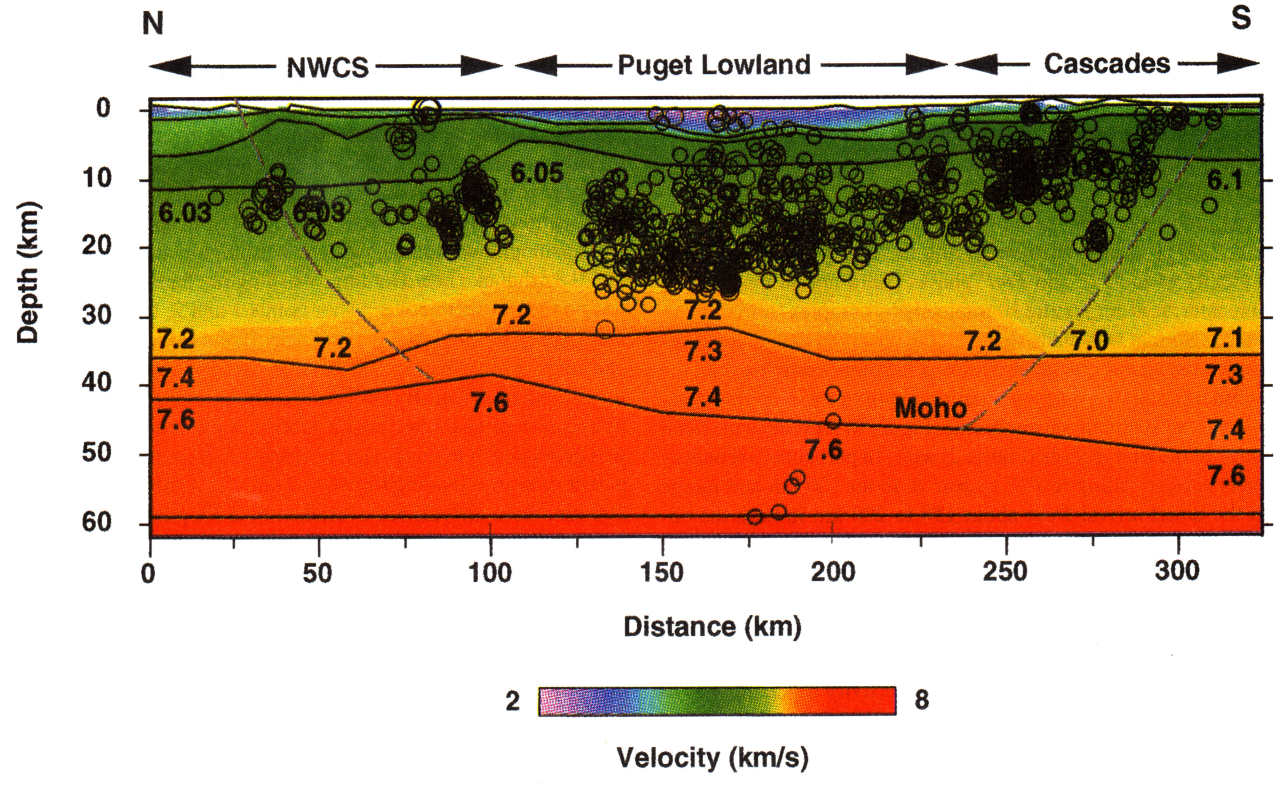

Plate 2. Crustal velocity model with earthquake hypocenters within 15 km of the seismic transect. Earthquakes are A or B quality events that occurred between 1970 and August 1994. Dashed gray lines indicate bounds on ray coverage for *PmP*.

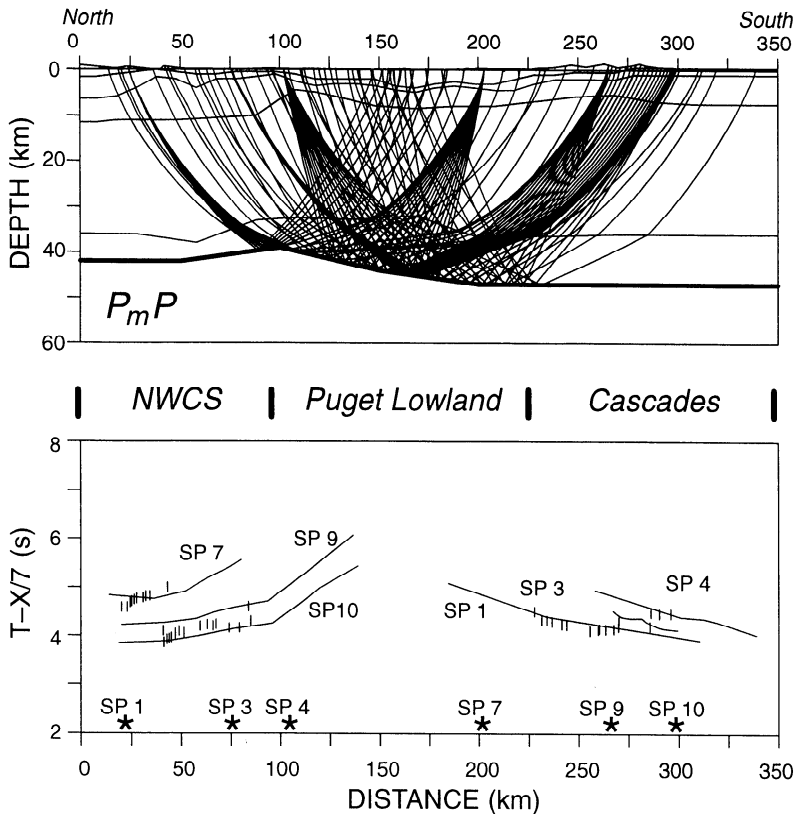

Figure 5. Ray trace diagram for the inversion of the *PmP* phase. Vertical bars are the observed travel times, and their height reflects the estimated uncertainty in the picks.

in the relatively thin layer above it. Thus the Moho geometry shown also has an uncertainty of about ± 2 km. The ray coverage indicated in Figures 4 and 5 should be remembered when viewing the model in Plate 2. For example, the 7.3–7.4 km s^{-1} layer does not have to be present north of about 75 km in model coordinates, and the results of profiling in southern Canada [*Zelt et al.*, 1993] indicate it is not present there.

Amplitude modeling using the reflectivity method [*Fuchs and Müller*, 1971] was used to verify the travel time modeling. The complexity of the *PlP* and *PmP* phases could not be matched by simple interfaces nor justified completely by complex source signatures. No attempt was made to model the observed data in great detail since the actual crustal structure is far more complex than the one-dimensional (1-D) approximation required by the reflectivity. However, the synthetic seismograms (Figure 6) reproduce the main features of the shot records (Figure 2) well. In particular, secondary arrivals corresponding to *PlP* appear at about 100 km and merge with the direct arrival from about 150 to 200 km in both the observed data and the synthetics. Also, the high-energy reflections arriving after the initial *PmP* pulse at offsets beyond 200 km on the shot records can be reproduced in the synthetic with alternating high- and low-velocity layers (7.2–7.5 km s^{-1}) in the lower 10 km of the crust. This layering also contributes to low *Pn* amplitude in the synthetic. The main result of the reflectivity modeling was to verify the velocity gradient from 10 to 35 km depth and to show that the 7.3 –7.4 km s^{-1} layer can be represented as a complex transition zone from lower crust to upper mantle.

The high amplitude of arrivals beyond ~150 km offset suggests to us that they are probably wide-angle reflections. However, if they are treated as refracted arrivals from the lower crust, in the *Hole* [1992] inversion, they produce an output velocity model that requires velocities of at least 7.2 km s^{-1} to depths of 42 to 46 km. This result is very similar to that obtained for the wide-angle interpretation, especially given the error estimates. Both approaches suggest that the crust–mantle boundary along the profile is extremely transitional.

In order to place a constraint on upper mantle velocity, two record sections (Figure 7) were constructed from earthquake sources and seismograms from the western Washington network. The 1991 *M* 5.0 earthquake near Deming, Washington, had an epicenter that lies on the transect between shot points 1 and 2, and a focal depth of 12 km. The 1993 *M* 5.6 event near Scotts Mills Oregon, had an epicenter approximately 100 km due south of shot point 10 and a focal depth of 20 km. By collecting seismograms from network stations adjacent to the refraction profile, a pseudo-reversed profile was generated. On these data, first arrivals from the crust have apparent velocities ranging from 6 to 7 km s^{-1}. At offsets greater than 200 km, these arrivals are overtaken by a *Pn* phase with apparent velocities of approximately 7.7 km s^{-1} which we adopt as the uppermost mantle velocity in our interpretation.

Forward modeling of the *Pn* arrival from the earthquake data (Figure 8) using the crustal velocity model obtained from the explosion data leads to an estimate of 7.6–7.8 km s^{-1} for the upper mantle velocity. The uncertainty in origin time for the earthquakes means that these data can not be used as a strong constraint on crustal thickness. However, we note that this modeling required no change in the crustal model obtained from the explosion data. In addition, it suggests that the crust probably thickens to nearly 50 km to the south (Figure 8).

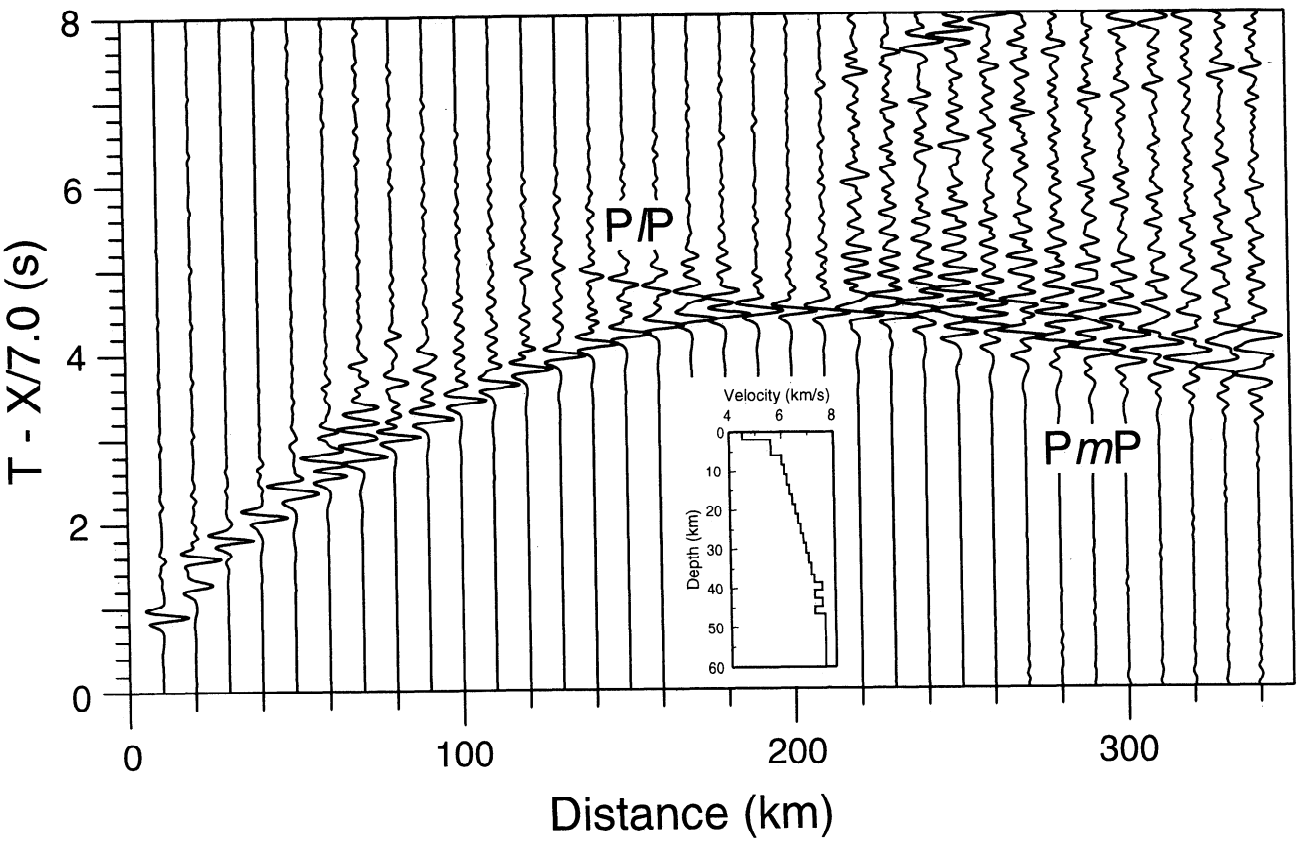

Figure 6. Modeled amplitude response for 1-D velocity model (inset) using reflectivity method. PlP is a discrete reflection. Reverberatory energy behind *PmP* result from interlayers of 7.2 and 7.5 km s^{-1} material in the lower crustal layer. *Pn* amplitudes are low due to the low-velocity contrast between the transitional lower crustal layer and the upper mantle.

Relationship of Upper Crustal Velocity Model to Geology

The seismic profile crosses three major geologic provinces in western Washington (Figure 1). To the north the transect crosses rocks of the pre-Tertiary continental framework, the Northwest Cascades Thrust System (NWCS). Near km 80 of the model (Plate 2), the line crosses the Darrington–Devils Mountain fault zone (DDMFZ) into the eastern flank of the Puget Lowland. Near kilometer 210 of the model, the profile leaves the Puget Lowland (Figure 1) and crosses into the Tertiary volcanic rocks of the Cascades. All three of these provinces have distinctive velocity characteristics in the upper 10 km of the crust. Below 10 km, variation in the depth to the 6.5 km s^{-1} contour points to changes in basement type across the region. In the following subsections, the velocity field in each province is discussed in light of its implications for regional geology.

Northwest Cascades Thrust System

The upper 10 km of the crust in the NWCS is dominated by velocities ranging from 4 to 5.5 km s^{-1} with at least two localized pods of material that approach 6.0 km s^{-1}. These velocities are consistent with rocks observed in the mapped geology which suggests that the upper crust is made up of at least two major thrust sheets composed of marine metasedimentary and metavolcanic rocks of Paleozoic age. The lower sheet, the Church Mountain thrust plate consists of volcanic and sedimentary rocks of the Devonian to Permian Chilliwack Group (volcaniclastic siltstone and sandstone, basaltic andesite breccias and tuffs). In the upper part of the sheet, a complex Imbricate Zone is found that contains the Yellow Aster Complex, a remnant of ancient continental crust, as well as fragments of tectonized and serpentinized alpine metaperidotites such as the Twin Sisters dunite. The upper sheet, the Shuksan thrust plate, is composed of the metabasaltic Shuksan Greenschist and the Darrington Phyllite [*Misch*, 1988]. At 5 km depth in the crust, rocks such as metagraywackes and serpentinites commonly have velocities of approximately 5.2 km s^{-1}, whereas phyllites and greenschist facies basalts exhibit velocities of 6.1 km s^{-1} and 6.7 km s^{-1} [*Christensen and Mooney*, 1995]. Thus when compared to the surface geology, the observed velocities suggest that the bulk of the NWCS crust is dominated by metasedimentary lithologies as well as serpentized basalts. Low velocities in the upper few kilometers can be attributed to the continued presence of fractures and significant levels of fluids in the rock.

The inversion defines localized pods of high velocity material at a depth of 4 km near km 40 of the model and at 2 km depth near km 80 of the model. Examination of the observed and calculated travel time curves (Figure 3) shows that the inversion probably underestimates velocities in this region. In both these regions, local travel time advances with apparent velocities near 7 km s^{-1} are poorly fitted by the calculated arrivals due to the smoothing apply in the inversion procedure. An attempt was made to fit these anomalies more precisely with forward ray tracing. The travel time advances can be fitted to within 0.1 s with two north dipping slabs of material

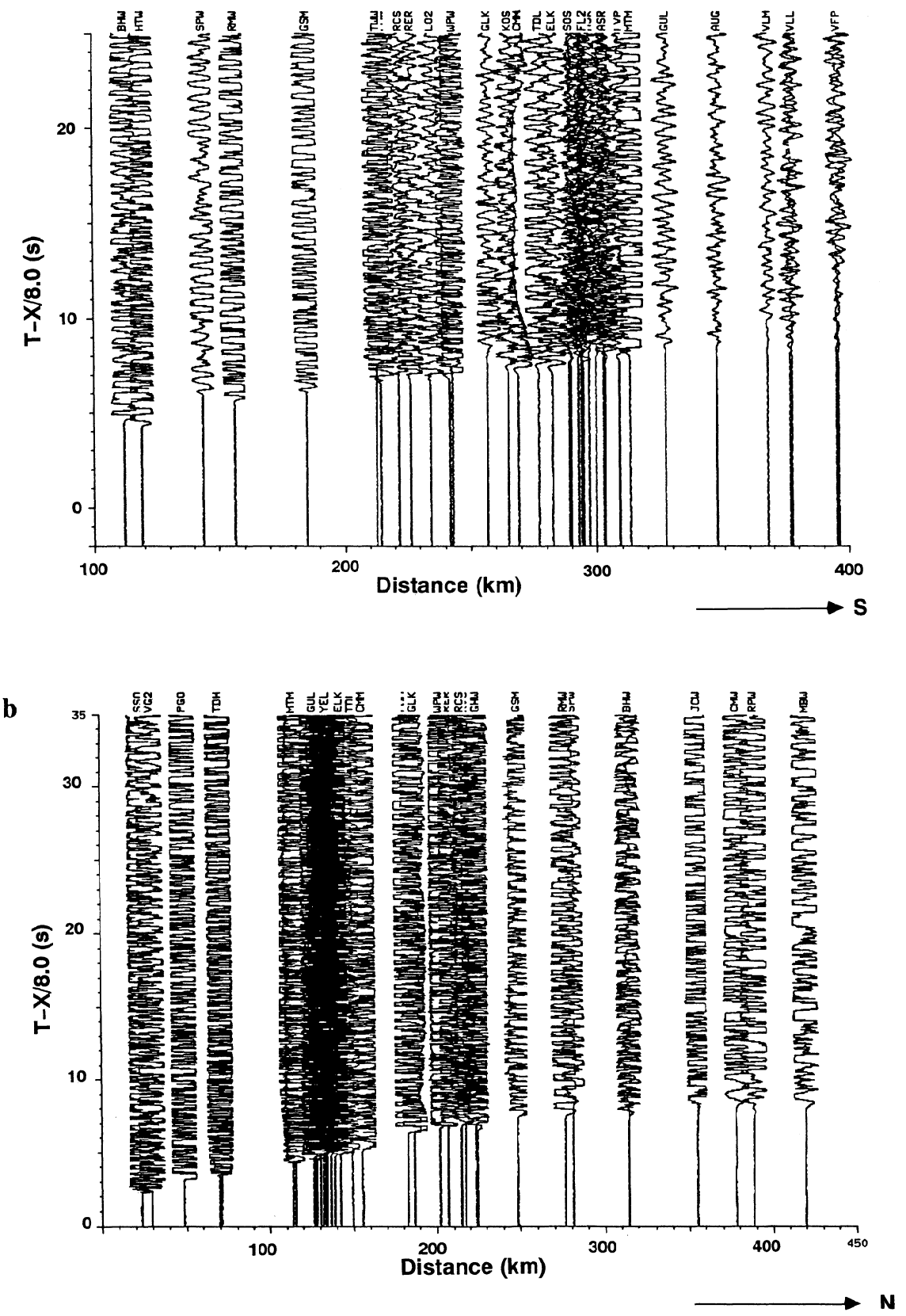

Figure 7. Earthquake record sections: (a) Deming and (b) Scotts Mills. Records are plotted with travel time reduced at 8 km s^{-1}.

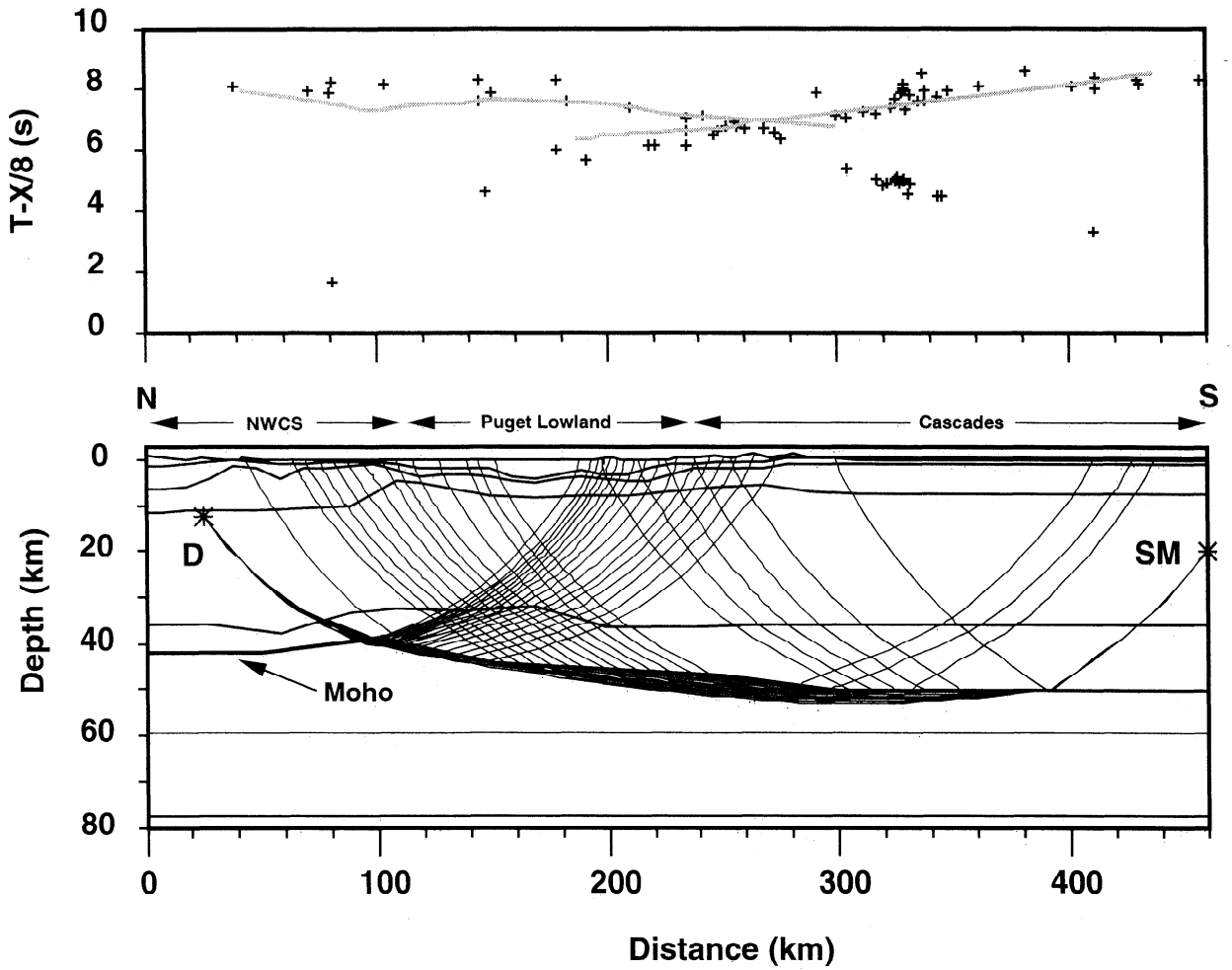

Figure 8. Earthquake raytrace diagram. D, Deming; SM, Scott Mills. Hypocenters are as reported in University of Washington earthquake catalog. Gray curves represent *Pn* arrivals calculated from the velocity model. Between 0 and 320 km, the crustal velocity model is the same as that obtained from the explosion model. A better match to the earthquake arrivals is obtained by thickening the crust south of 320 km.

with velocities of 6.2 to 6.8 km s^{-1}. The north dip on these bodies is consistent with southwest directed thrusting observed in the region. We interpret these to represent two slabs of mafic to ultramafic material entrained in the thrust sheet. Their size and geometry is consistent with other ophiolitic fragments observed in the region including the Twin Sisters dunite [*Thompson and Robinson,* 1975] located approximately 10 km east of shot point 2, Sumas Mountain, Haystack Mountain, and Table Mountain [*Whetten et al.,* 1980].

The velocity model suggests that the boundary between the NWCS and the Puget Lowland (Plate 1) is a steeply dipping fault. In the upper 4 km of the crust, near km 100 of the velocity model 4–5 km s^{-1} material of the NWCS is juxtaposed against 1.9–3.5 km s^{-1} rocks of the Puget Lowland. At 5–10 km depth, in the same location, NWCS rocks with velocities of 5.5 km s^{-1} are juxtaposed against 6.2 km s^{-1} material beneath the Puget Lowland. At the surface this transition is marked by the Darrington–Devils Mountain fault zone. This high-angle fault zone separates pre-Tertiary rocks of the NWCS from Tertiary strata to the south [*Tabor,* 1994]. The fault is inferred to have accommodated both dip-slip and strike-slip movement during Tertiary time [*Tabor,* 1994].

The Puget Lowland

The seismic line skirts the eastern flank of the Puget Lowland and thus presumably crosses through the more shallow reaches of the Everett and Seattle basins. The Puget Lowland lies between km 90 and 250 of the velocity model (Plate 1) and is characterized by 1 to 3.5 km of fill with velocities of 1.7 to 3.5 km s^{-1} that overlies a basement with velocities of 4.0 to 5.5 km s^{-1}. The transition between fill and basement is marked by a strong velocity gradient. Between km 90 and 160, where the profile skirts the eastern edge of the Everett basin, the basement interface dips gently southward at approximately 2° and then drops abruptly from 1.5 to 3.5 km depth over 20 km (5°) into the deepest part of the Seattle basin seen on this transect. South of the axis of the Seattle basin, this undulatory basement topography continues for another 30 km southward, where the basement interface begins to gradually climb from 2 km depth to the surface over 100 km (~ 1°).

The top of basement as defined here in the velocity model probably does not correspond to "tectonic" basement. That is, it probably does not correspond to either pre-Tertiary rocks or lower Eocene Crescent Formation on which marine sedimentary rocks of

Eocene age were deposited. Interpretation of seismic reflection data in Puget Sound, together with interval velocity estimates and sonic log data in wells tied to the reflection data [*Johnson et al.*, 1994; T. L. Pratt et al., Seismic reflection Images beneath Puget Sound, western Washington state: The Puget Lowland thrust sheet hypothesis, submitted to *Journal of Geophysical Research*, 1996, hereinafter referred to as Pratt et al., submitted manuscript, 1996] suggest that only Oligocene to Recent sediments in the basin have velocities less than 4.0 km s^{-1}. However, Eocene deposits appear to have velocities of 4.2 to 5.0 km s^{-1} [*Johnson et al.*, 1994]. Outcrops indicate that Eocene strata occur in the eastern portion of the Lowland [*Vine*, 1969; *Yount and Gower*, 1991], so the boundary in the velocity model may only represent the interface between Eocene sedimentary rocks and late Oligocene to Miocene strata. Since these velocities fall in the same range of values seen in the pre-Tertiary rocks of the NWCS, the velocity model probably can not be used by itself to differentiate between Tertiary sedimentary rocks, and basement rocks of the pre–Tertiary continental framework.

In its location on the eastern flank of the Puget Lowland, the seismic transect crosses a thinner section of sedimentary strata than has been previously documented in the central parts of the Everett and Seattle basins. Using seismic reflection data, *Johnson et al.* [1996] have estimated that as much as 6 km of sediment overlie basement in the Everett basin. Up to 4 km of this section belong Oligocene and younger strata. In the deepest parts of the Seattle basin, *Johnson et al.* [1994] estimated that 9 to 10 km of sediment rest on Crescent Formation basement in the Puget Sound . This estimate has been subsequently revised to 8 to 8.5 km based on new velocity analyses (T. L. Pratt, personal communication to S. Y. Johnson, 1995). Of this, 6 to 7 km belong to Oligocene and younger strata. Along the seismic refraction transect, up to 1.5 km of low (< 4 km s^{-1}) velocity material is observed in the Everett basin. This material probably corresponds to the Oligocene to Quaternary section that rests on pre-Tertiary basement there. A gravity model of the Everett basin [*Johnson et al.*, 1996] is consistent with this interpretation.

The southern margin of the Seattle basin, as seen on the velocity model (Plate 1), exhibits a very different geometry from the near-vertical boundary seen on seismic reflection records in Puget Sound [*Johnson et al.*, 1994; Pratt et al., submitted manuscript, 1996]. There, thrusting along the Seattle fault leads to 8–9 km of uplift of the Crescent Formation relative to the base of the Seattle basin. In a velocity model, this would appear as a near-vertical boundary juxtaposing material with velocities greater than 5.0 km s^{-1} with basin fill at less than 3.5 km s^{-1}. In contrast, the southern basin boundary in our velocity model appears as a gently (~ 1°) south dipping boundary. Outcrops of Paleogene sedimentary rocks just north of shot point 7 and misfits of the calculated travel time to the observed near km 190 of the model (Plate 1) hint that the basin boundary may be more complex than portrayed in the model. The outcrop demonstrates that Eocene sedimentary rocks have been brought to the surface by the Seattle fault [*Vine*, 1969; *Yount and Gower*, 1991]. The local advances in the observed travel time curves suggest that relatively fast material occurs near the surface but that this features is too localized for the inversion procedure to model in detail.

Cascades and the SWCC

The change in geology from the Puget Lowland to the Cascades is marked by the southward thinning of material with velocities less than 3.5–4.0 km s^{-1} in the upper few kilometers of the crust. South of km 250 in the model (Plates 1 and 2), the velocity model is laterally homogeneous and grades from velocities of 4.0 km s^{-1} near the surface to velocities of ~5.5 km s^{-1} at 6–7 km depth. Surface geology suggests that the seismic profile crosses both Eocene-Miocene sedimentary rocks (Puget Group), and late Eocene-to-Miocene age volcanic rocks of the Cascades. Between km 230 and 275 of the model, the seismic line traverses outcrops of folded and faulted Eocene nonmarine rocks (Puget Group), before crossing onto exposures of Tertiary volcanic rocks of the Cascades. No gradient in velocity accompanies this change in geology. This is not surprising, as velocities in these two groups of rocks are probably comparable [*Stanley et al.*, 1992, 1994; *Krehbeil*, 1993].

Within the Cascades, the seismic line crosses directly through a major conductivity anomaly, the Southern Washington Cascades Conductor (SWCC), defined by magnetotelluric surveys of the region [*Stanley et al.*, 1987, 1992]. This feature is a zone of low resistivity (2–5 ohm m) that is found at depths of 3–5 km and may extend to 10–20 km depth beneath the seismic profile. These very low resistivities led *Stanley et al.* [1987] to interpret this anomaly as representing marine sedimentary rocks of pre–Eocene to Eocene age, possibly indicative of an accretionary wedge/forearc basin caught between the Siletz terrane and the North American continent.

Below depths of 7 to 8 km where velocities exceed 5.5 km s^{-1}, it difficult to reconcile an entirely marine sedimentary origin for the SWCC with the velocity model. Seismic observations of velocities in well-consolidated mudstones and shales rarely exceed this value [e.g., *Christensen*, 1982]. Furthermore, well log data from analogous strata in western Washington rarely exceed this velocity [*Stanley et al.*, 1994]. Alternative explanations for the conductivity anomaly offered by *Stanley et al.* [1992] include: (1) altered volcanic ash flows made conductive through the development of authigenic minerals such as zeolites and smectites; (2) non–marine sedimentary rocks; (3) unmetamorphosed marine shales and mudstones of pre-Tertiary age; (4) presence of geothermal fluids and/or partial melt in the deeper part of the SWCC. Since, the velocity model appears to rule out sedimentary rocks of low metamorphic grade as an explanation for the SWCC at depth, the possibility that volcanic rocks or geothermal fluids contribute to the anomaly must be taken more seriously.

A Distinct Boundary Between Upper and Middle Crustal Rocks

A distinct change in velocity gradient at 6–11 km depth divides the upper crust from the middle crust in the model. Below this boundary, the middle crust is characterized by velocities grading from 6.1 km s^{-1} at the top to 7.2 km s^{-1} at its base near 34–38 km. As previously discussed, this interface is offset 7 to 10 km at km 100 of the model, suggesting that the DDMFZ that juxtaposes pre-Tertiary rocks and Tertiary rocks of the Puget Lowland extends at least into the middle part of the crust. This vertical offset also emplaces a 4-km-thick pod of high-velocity material beneath the Everett basin. Otherwise, the interface between the upper and middle crust is characterized by north dip of a little over 1°.

The most remarkable feature of the middle crust is an increase in mean crustal velocity in the southern part of the transect over the north. This can be seen most clearly where the 6.5 km s^{-1} contour steps up to 12–14 km from 19–20 km depth immediately beneath the Seattle basin (Plate 1). This results in an overall increase in velocity of 0.2–0.3 km s^{-1} in the south over the north. This rapid change suggests a significant change in basement composition.

The two main choices for basement in western Washington are the Siletz terrane and the pre-Tertiary continental basement. One explanation for the observed increase in midcrustal velocities is that a fragment of Siletzian basement underlies the transect south of the Seattle basin, whereas the northern section is underlain by pre-Tertiary continental rocks. If this interpretation is correct, it places Siletzian basement much farther to the east than previously thought.

The seismic velocity character of the Siletz terrane is well defined in the interpretation of the two 1991 wide-angle seismic transects in Oregon and southwestern Washington [*Tréhu et al.*, 1994]. In the coast ranges of southwestern Washington, where basalt of the Siletz terrane is seen in outcrop (Figure 1), velocities of 6.5 km s^{-1} are found at a depth of 6 km, and velocities of 7.0 km s^{-1} are found as shallow as 12 km. Thus this terrane is clearly defined by high seismic velocities, even in the uppermost crust.

The actual boundary between basaltic rocks of the Siletz terrane and pre-Tertiary continental rocks is largely buried beneath the Puget Lowland and the Tertiary volcanic pile in the Cascades but is thought to be a major strike-slip fault, termed the Puget Fault, that was active during Eocene time [*Johnson*, 1984]. A sub-vertical contact between the two blocks is inferred in part on the basis of strong north-south trending gravity and magnetic gradients. These mark a transition between gravity and magnetic highs associated with outcrop of basaltic rocks to the west and the gravity and magnetic lows to the east [e.g., *Finn*, 1990].

Consistent with this interpretation is the magnetotelluric (MT) model of *Stanley et al.* [1992] which shows the boundary between the Siletz terrane and the SWCC as a subvertical boundary. Likewise, *Finn* [1990] presents a gravity model in which a basaltic body with a density of 2920 kg m^{-3} is juxtaposed against marine sedimentary rocks of the SWCC with density of 2630 kg m^{-3}. Beneath the SWCC at 10–12 km depth, Finn's model includes a body with a density of 2855 kg m^{-3} which is comparable to the density used for the Siletz terrane and is significantly less than the 2720 kg m^{-3} density used to explain the observed gravity at comparable depths east of the SWCC. Thus this model lends additional support to the possibility that a fragment of the Siletz terrane may occur beneath the SWCC.

An alternative explanation for higher midcrustal velocities to the south is that the rocks of the pre–Tertiary continental framework are simply more mafic in this area than in the NWCS. This is certainly the case for results from Southern Cordillera Refraction Experiment (SCoRE) '89 line 3, immediately north of the border in Canada [*Zelt et al.*, 1993]. There, velocities of 6.5 km s^{-1} are reached at depths of 8–11 km.

Interpretation of Lower Crust and Upper Mantle Velocities

Even though the seismic profile in western Washington crosses diverse geologic provinces at the surface, the crustal thickness, middle-to-lower crustal velocities, and upper mantle velocity in the model are most characteristic of those observed in magmatic arcs. The most distinguishing characteristic of arc terranes is a thick, high-velocity lower crustal section [*Holbrook et al.*, 1992] observed in active, inactive, and exhumed arcs [*Miller and Christensen*, 1994]. Active arcs are also characterized by low *Pn* velocities. Along the western margin of the Cascades, crustal thickness ranges from 40 to 50 km. Velocities in the crust exceed 6.5 km s^{-1} at 20 km depth in the crust and exceed 7.0 km s^{-1} below 30 km. In addition, upper mantle velocities may be as low as 7.6 km s^{-1}.

Comparison of the western Washington results with those from a refraction experiment conducted entirely within the Oregon Cascades (Figure 9) [*Leaver et al.*, 1984] suggests that the Washington profile is largely the product of the processes associated with the active continental arc. The Leaver et al. model has nearly the same mean crustal velocity as our model, similar crustal thickness at ~ 42 km and a low *Pn* velocity of 7.7 km s^{-1}. The models differ slightly in the middle to lower crust in that Leaver et al. interpret low-velocity gradients between 10 and 30 km depth and then a jump from velocities of 6.6 to 7.0 km s^{-1} near 30 km depth. In the western Washington model, the lower crust is interpreted as a constant gradient to depths of ~ 37 km, where the transitional layer is encountered.

Laboratory studies of seismic velocity in rocks show that these high velocities, in a region with high heat flow, are characteristic of

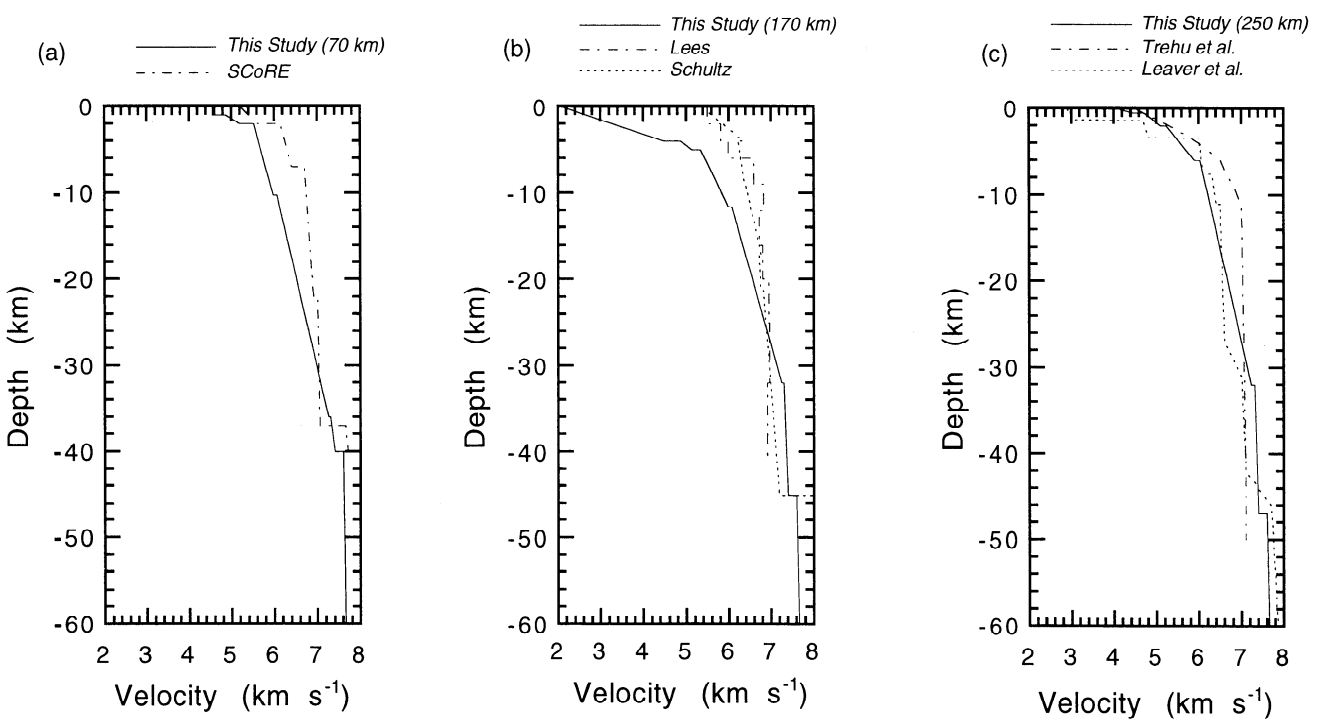

Figure 9. One-dimensional velocity models showing comparison between (a) this study and *Zelt et al.* [1993]; (b) this study, *Lees and Crosson* [1990], and *Schultz and Crosson* [1996]; c) this study, *Tréhu et al.* [1994], and *Leaver et al.* [1984].

a very limited suite of rock types. Assuming high heat flow, the primary candidates for rocks in the lower part of the crust are gabbro norite ($V_p = 6.9 \pm 0.25$ km s^{-1}) and mafic garnet granulite ($V_p = 6.8 \pm 0.2$ km s^{-1}) [*Christensen and Mooney,* 1995]. These types of rocks and velocities have also been observed and measured in the exhumed Kohistan arc [*Miller and Christensen,* 1994].

A transitional layer like the 5–10 km thick layer of 7.3–7.4 km s^{-1} material seen at the base of the crust in western Washington is commonly seen in seismic studies of rifts [e.g., *Thompson et al.,* 1989] but is difficult to explain in terms of typical crustal rock types at the elevated temperatures expected in the high heat flow regime of the Cascades arc. Some mafic rocks such as mafic garnet granulite or garnet gabbros have velocities in this range at room temperature, but at temperatures of 700–800 °C as might be expected in the lower crust of an active arc, the seismic velocity of these rocks are reduced by 0.3–0.4 km s^{-1} [*Christensen,* 1979]. Thus this temperature effect pushes them out of the range of typical candidate rock types for the lower crust. If ultramafic rock types alone are considered, we see that the temperature effect can not reduce velocities sufficiently to make them candidates for this layer. For example, laboratory measurements indicate the following velocities under these P–T conditions: in dunite, $V_p = 7.9$ km s^{-1}; in mafic eclogite, $V_p = 7.7$ km s^{-1}; and in pyroxenite, $V_p = 7.4$ km s^{-1}.

Models that can explain average velocities of 7.3–7.4 km s^{-1} include a transitional layer of interlayered mafic and ultramafic rocks, a gradation between mafic cumulates and ultramafic cumulates at the base of the crust, the presence of partial melt. For example, interlayering of 50% gabbro norite and 50% dunite leads to an average velocity of approximately 7.35 km s^{-1}. Models such as these that include layering are consistent with the seismic reflectivity modeling of the refraction data (Figure 6) which required high/low velocity layering within the transition layer to explain secondary arrivals in the data.

Alternatively, the lower crustal layer could actually be mantle material with a few percent (<5%) partial melt ponded at the base of the crust. Laboratory measurements show that just a few percent partial melt lead to a large decrease in P wave velocity [*Sato et al.,* 1989]. However, the observation that velocity does increase to 7.7 km s^{-1} in the upper mantle suggests that partial melt of mantle material is an unlikely explanation for observed velocities in the transition layer.

Examination of the base of the crust in an exhumed section of island arc in Pakistan offers a third explanation for the transition layer. In this section, the lowermost section of the crust is represented by 5 km of igneous garnet bearing gabbros that are underlain by a chemically contiguous suite of ultramafic cumulates. Laboratory velocities measurements on these rocks suggest that the seismic Moho is at a transition from ultramafic cumulates to mafic cumulates within a single coherent intrusion [*Miller and Christensen,* 1994]. A similar gradual change in composition would explain the velocity model we present here and perhaps presents evidence that crust–mantle boundary can be very gradual in active arcs.

The pseudo-reversing earthquake profiles show that the upper mantle velocity in western Washington is a low 7.6 km s^{-1}. This result is supported by other measurements of *Pn* in this region. Using a time-term method with local earthquake sources and stations in the local earthquake network, *Zervas and Crosson* [1986] obtained an average *Pn* velocity of 7.79 km s^{-1} west of the Cascades in Washington. They found that *Pn* was as low as 7.62 km s^{-1} at a location in the vicinity of km 280 of our velocity model and has high as 7.85 km s^{-1} near km 180 of the model. Previous workers including *Dehlinger et al.* [1965] have obtained similar results. More recently *Zelt et al.* [1993] have obtained an unreversed *Pn* velocity of 7.6 km s^{-1} along SCoRE line 3 in southern British Columbia. We interpret these low upper mantle velocities as a manifestation of high upper mantle temperatures that can reduce mantle velocities by as much as 5%. Partial melt may also contribute to low velocities in the upper mantle.

Comparison to Other Seismic Velocity Models

The western Washington velocity model can be placed in a more regional perspective in a comparison to other velocity models developed for southern British Columbia [*Zelt et al.,* 1993], western Washington [*Lees and Crosson,* 1990; *Schultz and Crosson,* 1996], and western Oregon [*Tréhu et al.,* 1994; *Leaver et al.,* 1984]. We have extracted representative 1-D velocity models from these models (Figure 9) as a basis for this discussion. Where velocity models have been developed from earthquake data, the refraction model should be viewed as a calibration point.

The upper 5 km of the crust in southern British Columbia as shown on SCoRE line 3 [*Zelt et al.,* 1993] is faster and lacks the lateral heterogeneity seen in Washington, but the structure of the middle to lower crust is quite similar to that in Washington. Below 12 km, velocities range from 6.6 to 7.1 km s^{-1}, and crustal thickness reaches 37 km at the longitude of the western Washington profile. The SCoRE line 3 model lacks the transitional layer at the base of the lower crust seen in Washington. The presence of the transitional layer leads to thickening of the crust to 41 km at the north end of the Washington profile. We suggest that this layer probably thins northward, such that at SCoRE line 3 the crustal mantle boundary is equivalent to the top of the transitional layer in Washington.

The most comprehensive velocity model for western Washington is a three–dimensional model derived from tomographic imaging of local earthquake delay times by *Lees and Crosson* [1990]. A direct comparison of a slice through this volume at –122° longitude with our velocity model shows that there are significant differences between the two models in the upper 10 km of the crust, but that the models are comparable in the middle to lower crust. In the upper 4 km of the crust the Lees and Crosson model shows velocities ranging from 5.4–6.0 km s^{-1}. The upper two layers of our model not only contain a much wider range of velocities (1.8–5.2 km s^{-1}), but these velocities are also much lower on average than those obtained from the tomography. Differences between the two models decrease in layer 3 of our model (~4–8 km) such that the velocities obtained in the tomography are only 0.3–0.5 km s^{-1} greater. By 15 km depth, the two models have velocities within 0.2 km s^{-1} of one another. Possible reasons for the large differences in upper crustal velocity structure include relatively sparse station coverage in the regional network, particularly in parts of the Puget Sound basin, and the effect of fixed station correction terms in the tomography.

A NW–SE trending two-dimensional crustal velocity model developed from earthquake sources [*Schultz and Crosson,* 1996] crosses the refraction model near km 240. At their intersection, both models have comparable middle to lower crustal velocities and crustal thickness (~ 45 km). Velocities in the upper 10 km of the Schultz and Crosson model are 0.4–1.0 km s^{-1} faster than in the refraction model. Velocity discrepancies between the two models decrease with depth.

As discussed above, refraction data from the Oregon Cascades [*Leaver et al.,* 1984] yield a velocity model very similar to that obtained in the Cascades reach of our transect, however, the dramatically different structure seen on the north end of PACNW–91 line 2 [*Tréhu et al.,* 1994], points to a substantial compositional change between these two regions. In the Coast Ranges of Washington and Oregon, *Tréhu et al.* [1994] obtain velocities of 7.0 km s^{-1} as shal-

low as 12 km. This appears to be the seismic signature of the Siletz terrane and is markedly different than the 6.3–6.5 km s^{-1} crust observed at comparable depths on our profile.

Regional Gravity Model

As a test of the degree to which our model agrees with other studies in the area, we constructed a regional gravity model (Figure 10) which extends northward to tie with the studies in the southwestern British Columbia and southward to the area of the Scott Mills earthquake. This model thus ties directly to the refraction profiles in Canada and to the Oregon profile of *Leaver et al.* [1984]. We went to considerable effort to pick those gravity readings from our data base which fell closest to the locations of our seismic recording stations. This was an important thing to do because of the 3-D nature of many features along the profile, and thus we used a modified version of the 2-1/2-dimensional gravity modeling approach of *Cady* [1980]. We assigned densities which were appropriate for the seismic velocities in each layer; however, we have not tried to model every detail of the gravity profile. A simple structure which does vary much lateraly provides a tie to the Oregon model of *Leaver et al.* [1984] while honoring the travel-time model derived from the Scott Mill earthquake (Figure 8). A more complex structure was required on the northern end of the model. Here complexities revealed in a 3–D tomographic analysis of the Canadian data [*Zelt et al.*, 1996] had to be included in our model. In particular, the large midcrustal body in our model approximates a high-velocity region which is detected by the Canadian workers [*Zelt et al.*, 1993, 1996]. This feature is associated with a circular gravity high which our profile crossed. The ophiolite body at about 150 km in model coordinates is a detail which correlates well with our seismic modeling. In summary, the gravity model provides a more regional picture of the crustal structure and confirms that our seismic model ties well with other results in the area.

Correlation to Regional Seismicity Patterns

Seismicity in western Washington is characterized by abundant microearthquakes in the crust. When A or B quality events within 15 km of the seismic transect are culled from the University of Washington catalog (Plate 2), one can see that distinct seismicity patterns can be associated with the individual tectonic provinces along the seismic transect. In the NWCS and Puget Lowland, most of the seismicity occurs below the base of the upper crust as defined by a seismic boundary at 5–10 km depth and continues to 20–30 km depth. The region of transition between the NWCS and the Puget Lowland appears as a gap in seismicity with notably less seismic activity to the north than south of the boundary between the two. Earthquakes within the Cascades are generally shallower (0–20 km) and are dominated by events associated with the Rainier Seismic Zone which lies to the east of the profile and is subparallel with it.

Conclusions

Interpretation of new seismic data from western Washington state yields new insight into the crustal structure of the region. In the upper crust, major velocity boundaries are associated with tectonic boundaries defined at the surface. In particular, the boundary between the pre-Tertiary rocks of the NWCS and the Puget Low-

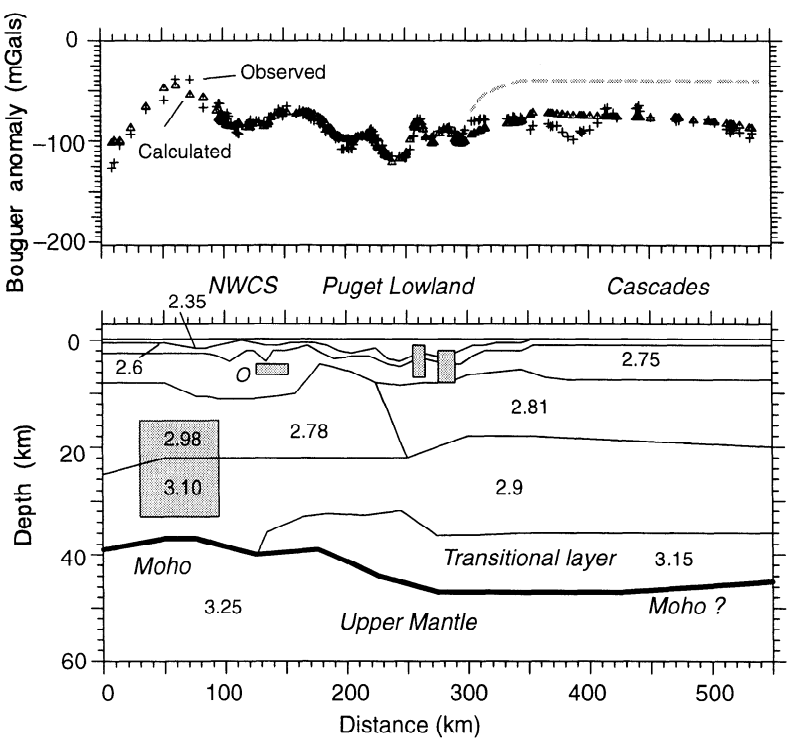

Figure 10. North–south gravity model through western Washington. The model trends due south of shot point 10 and ends at the same latitude as the Scotts Mills earthquake (Figure 1). Kilometer 100 on this model corresponds to 0 km on the velocity models. Numbers are densities in kg m^{-3} x 10^{-3}. O, ophiolite, 2.9. Other shaded bodies are mafic intrusions, 2.9. Dashed gray curve represents the calculated gravity that results from replacing the transitional layer with density 3.15 with mantle material at 3.25. The 50 mGal mismatch with preferred model substantiates the interpretation of thick crust to the south.

land is marked by a sub-vertical boundary in the velocity model that corresponds to the Darrington–Devils Mountain fault zone. An undulating basement topography overlain by low-velocity sediments (1.7–3.5 km s^{-1}) characterizes the Puget Lowland. The southern Washington Cascades are characterize by upper crustal velocities range from 4.0 to 5.5 km s^{-1} and reflect the large volume of Tertiary volcanics and sediments found in that region.

Below 10 km, crustal velocities are most similar to those seen in other active continental arcs. Between 10 and 35 km, the velocity field is characterized by a gradient from ~6.0–7.2 km s^{-1}, and is underlain by a 2–8 km thick transitional layer at the base of the with velocities of 7.3–7.4 km s^{-1}. These high velocities do not support the interpretation that the SWCC is caused by marine sedimentary rocks at depths of 10–20 km beneath the Cascades. Crustal thickness ranges from 42 to 47 km along the profile and the upper mantle velocity appears to be an unusually low 7.6–7.8 km s^{-1}. The transitional layer at the base of the crust appears to be layered and may consist of interlayered mafic and ultramafic rocks and/or the presence of partial melt. The unusually low upper mantle velocities may be due to high upper mantle temperatures, possibly accompanied by partial melt.

The observed crustal structure along this profile is distinctly different from that seen in the Coast Ranges of western Washington [*Tréhu et al.*, 1994], which lies almost entirely within the basaltic rocks of the Siletz terrane, but is quite similar to that seen in the Oregon Cascades [*Leaver et al.*, 1984]. The analysis of a recently acquired east–west transect in western Washington [*Luetgert et al.*, 1995], is required to fully understand the tectonic relationship of the Siletz block to Puget Lowland and the Cascades.

Acknowledgments. We thank the many people who participated in the permitting and acquisition of the data. We thank Steve Malone for providing record sections for the earthquake recordings, and R. Crosson, A. Tréhu, and the associate editor for helpful reviews. Research supported by the U.S. Geological Survey (USGS), Department of the Interior under USGS award numbers 14–08–0001–G2073 and 1434–95–G–2636. The views and conclusions contained in this document are those of the authors and should not be interpreted as necessarily representing the official policies, either expressed or implied of the U.S. Government.

References

Atwater, B. F., Evidence for great Holocene earthquakes along the outer coast of Washington State, *Science*, *236*, 942–944, 1987.

Blakely, R J., and R. C. Jachens, Volcanism, isostatic residual gravity, and regional tectonic setting of the Cascade Volcanic Province, *J. Geophys. Res.*, *95*, 19,439–19,451, 1990.

Brandon, M. T., and A. R. Calderwood, High-pressure metamorphism and uplift of the Olympic subduction complex, *Geology*, *18*, 1252–1255, 1990.

Cady, W. J., Calculation of gravity and magnetic anomalies of finite-length right polygonal prisms, *Geophysics*, *45*, 1507–1512, 1980.

Cady, W.M., Tectonic setting of the Teriary volcanic rocks of the Olympic Peninsula, Washington: *U.S. Geol. Surv. J. Res.*, *3*, 573–582, 1975.

Cerveny, V., I. Molotkov, and I. Psencik, *Ray Method in Seismology*, University of Karlova, Prague, Czech Republic, 1977.

Christensen, N. I., Compressional wave velocities in rocks at high temperatures and pressures, critical thermal gradients, and crustal low-velocity zones, *J. Geophys. Res.*, *84*, 6849–6857, 1979.

Christensen, N. I., Seismic velocities, in *Handbook of Physical Properties of Rocks*, vol. 2, edited by R. S. Carmichael, pp. 1–228, CRC Press, Boca Raton, Fla., 1982.

Christensen, N. I., and W. D. Mooney, Seismic velocity structure and composition of the continental crust: A global view, *J. Geophys. Res.*, *100*, 9761–9788, 1995.

Crosson, R. S., Crustal modeling of earthquake data, 2, Velocity structure of the Puget Sound region, Washington, *J. Geophys. Res.*, *81*, 3047–3054, 1976.

Dehlinger, P. E., F. Chiburis, and M. M. Collver, Local travel time curves and their geologic implications for the Pacific Northwest states, *Bull. Seismol. Soc. Am.*, *55*, 587–607, 1965.

Finn, C., Geophysical contraints on Washington convergent margin structure, *J. Geophy. Res.*, *95*, 19,533–19,546, 1990.

Fuchs, K., and G. Müller, Computations of synthetic seismograms with the reflectivity method and comparison with observations, *Geophys. J. R. Astron. Soc.*, *23*, 417–433, 1971.

Fuis, G. S., J. J. Zucca, W. D. Mooney, and B. Milkereit, A geologic interpretation of seismic–refraction results in northeastern California, *Geol. Soc. Am. Bull.*, *98*, 53–65, 1987.

Gonzalez, R. C., and P. Wintz, *Digital Image Processing*, Addison-Wesley, 503 pp., Reading, Mass., 1987.

Gridley, J. M., Crustal structure of western Washington, Ph.D. dissertation, Univ. Tex. at El Paso, 1993.

Holbrook, W. S., W. D. Mooney, and N. I. Christensen, The seismic velocity structure of the deep continental crust, in *Continental Lower Crust*, edited by D. M. Fountain, R. Arculus, and R. W. Kay, pp. 1–43, Elsevier, New York, 1992.

Hole, J. A., Non-linear high-resolution three-dimensional seismic travel time tomography, *J. Geophys. Res.*, *97*, 6553–6562, 1992.

Johnson, S. Y., Evidence for a margin-truncating transcurrent fault (pre-late Eocene) in western Washington, *Geology*, *12*, 538–541, 1984.

Johnson, S. Y., C. J. Potter, and J. M. Armentrout, Origin and evolution of the Seattle fault and Seattle basin, Washington, *Geology*, *22*, 71–74, 1994.

Johnson, S. Y., C. J. Potter, J. M. Armentrout, J. J. Miller, C. Finn, and C. S. Weaver, The southern Whidbey Island fault: An active structure in the Puget Lowland, Washington, *Geol. Soc. Am. Bull.*, *108*, 334–354, 1996.

Krehbiel, S., Depth estimates of seismic reflection data in SW Washington, *Leading Edge*, *12*, 1076–1081, 1993.

Leaver, E. W., W. D. Mooney, and W. M. Kohler, A seismic refraction study of the Oregon Cascades: *J. Geophys. Res.*, *89*, 3121–3134, 1984.

Lees, J. M., and R. S. Crosson, Tomographic imaging of local earthquake delay times for three-dimensional velocity variation in western Washington, *J. Geophys. Res.*, *95*, 4763–4776, 1990.

Ludwin, R. S., C. S. Weaver, and R. S. Crosson, Seismicity of Washington and Oregon, in *Neotectonics of North America Decade Map vol. I*, edited by D. B. Slemmons, E. R. Engdahl, M. D. Zoback, and D. D. Blackwell, pp. 77–98, Geol. Soc. of Am., Boulder, Colo., 1991.

Luetgert, J. H., Interactive two-dimensional seismic raytracing for the Macintosh, *U.S. Geol. Surv. Open File Rep.*, *92-356*, 1992.

Luetgert, J., W. Mooney, A. Tréhu, J. Nabelek, G. R. Keller, K. Miller, I. Asudeh, and B. Isbell, Data report for a seismic refraction/wide-angle reflection investigation of the Puget Basin and Willamette Valley in western Washington and Oregon, *U.S. Geol. Surv. Open File Rep.*, *93-347*, 1993.

Luetgert, J., T. Parsons, K. Miller, G. R. Keller, A. Tréhu, S. Fleming, R. Clowes, and I. Asudeh, Crustal architecture of the Pacific Northwest: The 1995 seismic transect across southern Washington, *EOS*, 76, F399, 1995

McBirney, A.R., Volcanic evolution of the Cascades Range, *Annu. Rev. Earth Planet. Sci.*, *6*, 437–456, 1978.

Miller, D. J., and N. I. Christensen, Seismic signature and geochemistry of an island arc: A multidisciplinary study of the Kohistan accreted terane, northern Pakistan, *J. Geophys. Res.*, *99*, 11,623–11,642, 1994.

Misch, P., Tectonic and metamorphic evolution of the northern Cascades: An overview, in *Metamorphism and Crustal Evolution of the Western United States*, edited by W. G. Ernst, pp. 179–185, Prentice Hall, Englewood Cliffs N. J., 1988.

Mooney, W. D., and R. Meissner, Continental crustal evolution observations, *Eos*, *72*, 537 –541, 1991.

Mooney, W.D., and C. S. Weaver, Regional crustal structure and tectonics of the Pacific coastal states; California, Oregon and Washington, in *Geophysical Framework of the Continental United States*, edited by L. C. Pakiser and W. D. Mooney, *Mem. Geol. Soc. Am.*, *172*, 129–161, 1989.

Sato, H., I. S. Sacks, and T. Murase, The use of laboratory velocity data for estimating temperature and partial melt fraction in the low-velocity

zone: Comparison with heat flow and electrical conductivity studies, *J. Geophys. Res., 94,* 5689–5704, 1989.

Schultz, A. P., A 2–D velocity structure for a cross–Cascades profile using earthquake sources, M. S. thesis, 55 pp., Univ. of Wash., Seattle, 1993.

Schultz, A. P. and R. S. Crosson, Seismic velocity structure across the central Washington Cascade Range from refraction interpretation with earthquake sources, *J. Geophys. Res., 101,* 27,899–27,915, 1996.

Snaveley, P. D., Jr., N. S. MacLeod, and H. C. Wagner, Tholeitic and alkalic basalts of the Eocene Siletz River volcanics, Oregon Coast Range, *Am. J. Sci., 266,* 454–481, 1968.

Stanley, W. D., C. Finn, and J. L. Plesha, Tectonics and conductivity structures in the southern Washington Cascades, *J. Geophys. Res., 92,* 10,179–10,193, 1987.

Stanley, W. D., W. J. Gwilliam, G. Latham, and K. Westhusing, The southern Washington Cascade conductor – A previously unrecognized thick sedimentary sequence, *AAPG Bull., 76,* 1569–1585, 1992.

Stanley, W. D., S. Y. Johnson, and V. F. Nuccio, Analysis of deep seismic reflection and other data from the southern Washington Cascades, *U.S. Geol. Surv. Open File Rep., 94-159,* 1994.

Taber, J. J., and T. R. Lewis, Crustal structure of the Washington continental margin from refraction data, *Bull. Seismol. Soc. Am., 76,* 1011–1024, 1986.

Tabor, R.W., Age of Olympic metamorphism, Washington; K-Ar dating of low-grade metamorphic rocks, *Geol. Soc. Am. Bull., 83,* p. 1805–1816, 1972.

Tabor, R. W., Late Mesozoic and possible early Tertiary accretion in western Washington state: The Helena-Haystack melange and the Darrington–Devils Mountain fault zone, *Geol. Soc. Am. Bull., 106,* 217–232, 1994.

Thompson, G. A., and R. Robinson, Gravity and magnetic investigation of the Twin Sisters dunite, northern Washington, *Geol Soc. Am. Bull., 86,* 1413–1422, 1975.

Thompson, G. A., R. Catchings, E. Goodwin, S. Holbrook, C. Jarchow, C. Mann, J. McCarthy, and D. Okaya, Geophysics of the western Basin and Range Province, in *Geophysical Framework of the Continental United States,* edited by L. C. Pakiser, and W. D. Mooney, *Mem. Geol. Soc. Am., 172,* 177–203, 1989.

Tréhu, A. M., I. Asudeh, T. M. Brocher, J. H. Luetgert, W. D. Mooney, J. L. Nabelek, and Y. Nakamura, Crustal architecture of the Cascadia forearc, *Science, 266,* 237–243, 1994.

Vidale, J., Finite-difference calculation of travel times in three dimensions, *Geophysics, 55,* 521–526, 1990.

Vine, J. D., Geology and coal resources of the Cumberland, Hobart and Maple Valley quadrangles, King County, Washington, *U.S. Geol. Surv. Prof. Pap., 624,* 27 pp., 1969.

Wells, R. E., Paleomagnetic rotations and Cenozoic tectonics of the Cascade Arc, Washington, Oregon, and California, *J. Geophys. Res., 95,* 19,409–19,417, 1990.

Whetten, J. T., R. E. Zartman, R. J. Blakley, and D. L. Jones, Allochthonous Jurassic ophiolite in northwest Washington, *Geol. Soc. Am. Bull., 91,* 359–368, 1980.

Yount, J. C., and H. D. Gower, Bedrock geologic map of Seattle 30' by 60' quadrangle, *U. S. Geol. Surv. Open File Rep., 91-147,* 37 pp., 5 sheets, scale 1:100,000, 1991.

Zelt, B. C., R. M. Ellis, and R. M. Clowes, Crustal velocity structure in the eastern Insular and southernmost Coast belts, Canadian Cordillera, *Can. J. Earth Sci., 30,* 1014–1027, 1993.

Zelt, B. C., R. M. Ellis, R. M. Clowes, and J. A. Hole, Inversion of three-dimensional wide-angle seismic data from the southwestern Canadian Cordillera, *J. Geophys. Res., 101,* 8503–8529, 1996.

Zelt, C. A., and R. B. Smith, Seismic traveltime inversion for 2-D crustal velocity structure, *Geophys. J. Int., 108,* 16–34, 1992.

Zervas, C. E., and R. S. Crosson, *Pn* observation and interpretation in Washington, *Bull. Seismol. Soc. Am., 76,* 521–546, 1986.

J. M. Gridley, G. R. Keller, and K. C. Miller, Department of Geological Sciences, University of Texas at El Paso, El Paso, TX 79968–0555. (e–mail: miller@geo.utep.edu).

J. H. Luetgert and W. D. Mooney, U.S. Geological Survey, 345 Middlefield Road, MS 977, Menlo Park, CA 94025. (e–mail: luetgert@andreas.wr.usgs.gov)

H. Thybo, Geological Institute, University of Copenhagen, Oster Voldgrade 10 DK 1350 Copenhagen, Denmark. (email: ht@seis.geol.ku.dk)

(Received August 15, 1996; revised February 20, 1997;
accepted March 17, 1997.)